**Proceedings of the 9ICEG**
9th International Congress on Environmental Geotechnics
25-28 June, 2023 | Chania, Greece
© Authors: All rights reserved, 2023
https://doi.org/10.53243/ICEG2023-83

# Satellite-based Change Detection for Mining Instability

Jhih-Rou Huang[1] and Dimitrios Zekkos[2]

[1]*Graduate Student, University of California, Berkeley, United States, email: jhihrou_huang@berkeley.edu*

[2]*Professor, University of California, Berkeley, United States, email: zekkos@berkeley.edu*

## ABSTRACT

Mining operations can generate a large amount of waste material, usually disposed of in tailings dams. Historical as well as recent tailings dam failures have shown that these facilities remain vulnerable and are prone to catastrophic failures. Remote sensing data can be utilized to regularly and remotely monitor the condition of operational and abandoned mining sites. This study aims to detect tailings dam instabilities using high-resolution satellite imagery and evaluate the performance of different remote sensing indexes in change detection for two recent study cases: the 2022 Jagersfontein tailings dam failure in South Africa and the 2019 Córrego de Feijão tailings dam failure event in Brazil. Vegetation and geological indexes derived from images are used to track spatial and temporal change at mining sites. It is shown that remote sensing indexes are good indicators of failure, but some indexes are better than others, depending on the site conditions. For the Córrego de Feijão tailings dam that is located in a vegetated area, the failure resulted in more than 0.1 change in the statistical mode of all remote sensing indexes differences. The Normalized Difference Vegetation Index (NDVI) difference performed best, with the highest change of 0.26. On the other hand, the Jagersfontein tailings dam, located in a non-vegetated area, resulted in a 0.07 change in the statistical mode of the Modified Triangular Vegetation Index (MTVI2) difference but had very little change in the other remote sensing indexes.

*Keywords: Mining Instability, Change Detection, Remote Sensing Indexes, Tailings Dam Failure*

## 1 INTRODUCTION

Mining activities produce a large amount of waste material, such as crushed rock, processed water, and chemicals (Kossoff et al., 2014). These waste materials are usually stored against human-made embankments known as tailings dams (Lyu et al., 2019). Billions of tons of mine tailings have been generated by the mining industry globally (Owen et al., 2020), and the decreasing ore grades show that vast amounts of tailings will need to be stored in the future (Bowker and Chambers, 2017).

Tailings dams are vulnerable to failure due to high maintenance costs during the operation and after mine closure (Rico et al., 2008). The tailings dam failure can affect areas several km away from the dam and adversely impact the environment. The rate of tailings dam failure was estimated to be approximately 1.2% in the last 100 years (Azam and Qiren, 2010), which is a higher failure rate than water retention dams (Bowker and Chambers, 2015). Islam and Murakami (2021) pointed out that the number of tailings failure events is rising, and the location of dam failures has shifted from developed to developing countries. Most small failure events are also underreported (Villarroel et al., 2006). Even though tailings dam failure is preventable, failures reoccur due to the lack of careful regulation (Yangon, 2020) and oversight.

Recent advances in remote sensing techniques and data availability have increased the value of remote sensing technologies in disaster response (Metternicht et al., 2005). For example, Mura et al. (2018) used DInSAR to monitor the vulnerability of dams and dikes after the collapse of the tailings dam of Fundao. Rudorff et al. (2018) analyzed the collapse of an iron ore mining wastewater dam using Landsat imagery. Rauhala et al. (2017) conducted unmanned aerial vehicle surveillance of a mine tailings impoundment in sub-arctic conditions. Remote sensing techniques have been applied to study mining activities but have yet to become standard practice. Also, most research focus has been on using satellite data to analyze a specific failure event rather than developing a system-level monitoring system for the mining sites.

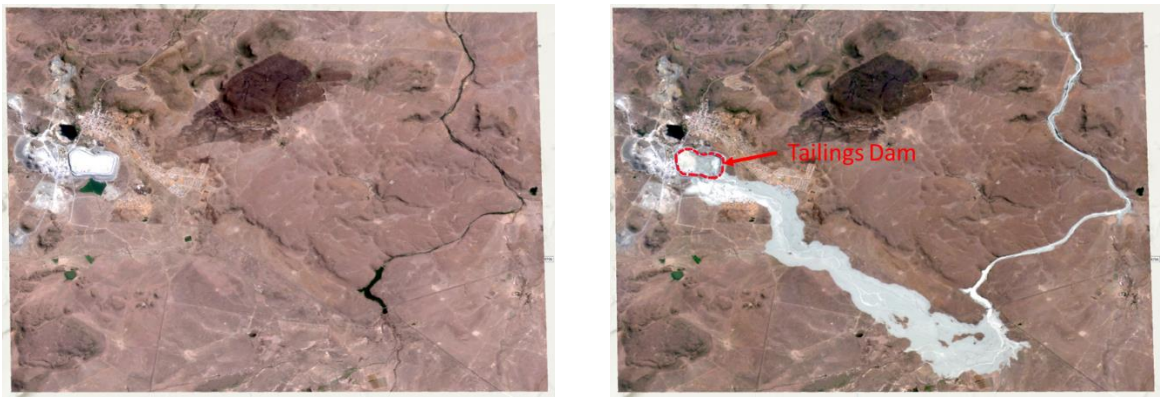
This paper presents the application of satellite-based change detection to detect the tailings dam instability in two recent failure cases: the 2022 Jagersfontein tailings dam failure (Motsau and Van Wyk, 2022) and the 2019 Córrego De Feijão tailings dam failure (Robertson et al., 2019). The goal is to quantify the change in remote sensing indexes that can be used to detect failures. Identifying the optimum detection indexes and their threshold values can be used as a reference to assess the condition of the tailings dam and detect or even prevent failures.

## 2 METHODOLOGY

### 2.1 Study Cases

The Jagersfontein mine is the deepest hand-excavated mine in the world and is known for Excelsior Diamond and Reitz Diamond (Streeter, 1892). On September 11, 2022, the Jagersfontein tailings dam collapsed. Fig 1(a) shows the Jagersfontein tailings dam before the 2022 failure. Fig 1(b) shows that the slide had a significant runout and affected a large downstream area after the failure. The tailings runout was about 1.5 km wide and extended 8.5 km toward the southeast (NASA Earth Observatory, 2022). The Jagersfontein tailings dam had a steep tailing gradient and was built on top of a shallow aquifer with steep retaining walls on a slope, all of which contributed to the failure (Motsau and Van Wyk, 2022).

Córrego de Feijão mine near Brumadinho, Região in Brazil, had a catastrophic rotational failure and released around 12 million cubic meters of ore tailings into the river on January 25, 2019 (Grebby et al., 2021). Fig 2(a) is a satellite imagery of the Córrego de Feijão mine before the failure. Fig 2(b) shows that the fluidized mass travelled approximately 10 km downstream and reached the river. The fluidized mass destroyed a bridge and led to 260 deaths. In addition, it contaminated the drinking water and damaged the habitat. Robertson et al. (2019) mentioned that liquefaction and vertical subsidence occurred before the dam collapsed. The lack of internal drainage, the steep upstream constructed slope, and rainfall were attributed as causes of the instability.




*(a) September 9, 2022 (pre-failure)* *(b) September 12, 2022 (post-failure)*

***Figure 1.*** *2022 Jagersfontein tailings dam failure, Planet Scope Scene Imagery*




*(a) January 24, 2019 (pre-failure)* *(b) February 1, 2019 (post-failure)*

***Figure 2.*** *2019 Córrego de Feijão tailings dam failure, Planet Scope Scene Imagery*

### 2.2 Data

Planet.com (Planet Team, 2017) provides global coverage of daily imagery from different sensors. Satellite imagery in different time frames was collected considering cloud coverage and image quality for the 2022 Jagersfontein tailings dam failure and the 2019 Córrego de Feijão tailings dam failure before and after the failure (see Table 1). We used the Planet Scope Scene, which has 3 m resolution with four bands, to evaluate and detect the change in the remote sensing indexes. As shown in the first line of Table 1, two images were used before the event to track the differences in the indexes under "normal" operations, whereas an image before and an image after were used to see the differences in indexes associated with the failure (as shown in the second line of Table 1).

***Table 1.*** *Satellite Imagery collected for change detection analysis*

| | 2022 Jagersfontein tailings dam failure (Duration between two images) | 2019 Córrego de Feijão tailings dam failure (Duration between two images) |
|---|---|---|
| Change detection before the failure | 09/04/2022 and 09/09/2022 (5 days) | 12/20/2018 and 01/24/2019 (1 month) |
| Change detection for the failure event | 09/09/2022 and 09/12/2022 (3 days) | 01/24/2019 and 02/01/2019 (9 days) |

### 2.3 Change Detection

Optical characteristics derived from satellite images were utilized in the model. Five remote sensing indexes were assessed and compared. Several indexes primarily related to vegetation were used and are shown in Equations (1)-(4): Normalized Difference Vegetation Index (NDVI), Green Normalized Difference Vegetation Index (Green NDVI), Visible Atmospherically Resistant Index (VARI), and Modified Triangular Vegetation Index (MTVI2). NDVI (Pettorelli, 2013) is the most used vegetation index using the red and near-infrared (NIR) band (Equation 1). The NIR band can distinguish the high reflectivity of vegetation, and the red band can show the chlorophyll pigment absorption. Green NDVI (Moges et al., 2005) is used to estimate photosynthetic activity (Equation 2). VARI (Stow et al., 2005) is a vegetation index that utilizes three visible bands to reduce the atmospheric effect (Equation 3). MTVI2 (Haboudane et al., 2004) detects the leaf chlorophyll content (Equation 4). Finally, Iron Oxide (IO) in Equation (5), a geological index, can detect rock experiencing oxidation of iron-bearing sulfides (Dogan, 2009). Change detection was performed in ArcGIS Pro 2.9.0 by calculating the pixel value change between two rasters at different times in Equation (6).

$$\text{Normalized Difference Vegetation Index (NDVI)} = \frac{\text{NIR}-\text{Red}}{\text{NIR}+\text{Red}} \quad (1)$$

$$\text{Green Normalized Difference Vegetation Index (Green NDVI)} = \frac{\text{NIR} - \text{Green}}{\text{NIR} + \text{Green}} \quad (2)$$

$$\text{Visible Atmospherically Resistant Index (VARI)} = \frac{\text{Green} - \text{Red}}{\text{Green} + \text{Red} - \text{Blue}} \quad (3)$$

$$\text{Modified Triangular Vegetation Index (MTVI2)} = \frac{1.5(1.2(\text{NIR}-\text{Green})-2.5(\text{Red}-\text{Green}))}{\sqrt{(2\,NIR+1)^2-(6\,NIR-5\sqrt{Red})}-0.5} \quad (4)$$

$$\text{Iron Oxide (IO)} = \frac{Red}{Blue} \quad (5)$$

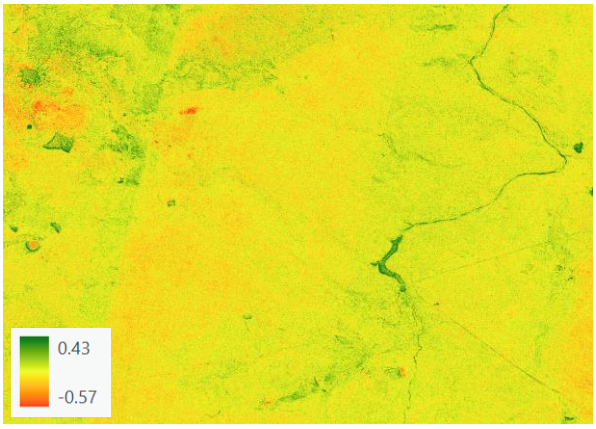
Where NIR is the near-infrared band; Red is the red band; Green is the green band; Blue is the blue band.

$$Remote\ Sensing\ Index\ Difference = Remote\ Sensing\ Index_{time2} - Remote\ Sensing\ Index_{time1} \quad (6)$$

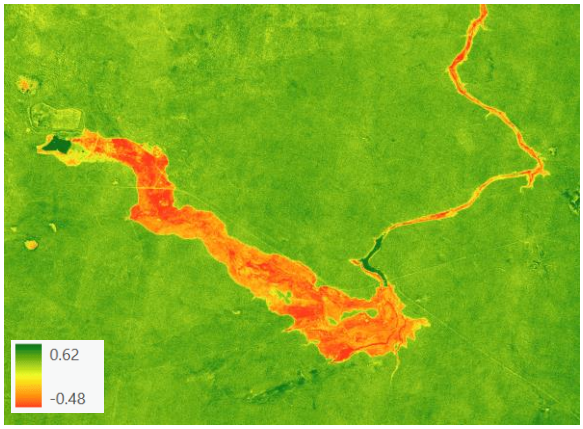
Where time 1 is earlier than time 2.

## 3 RESULTS AND DISCUSSION

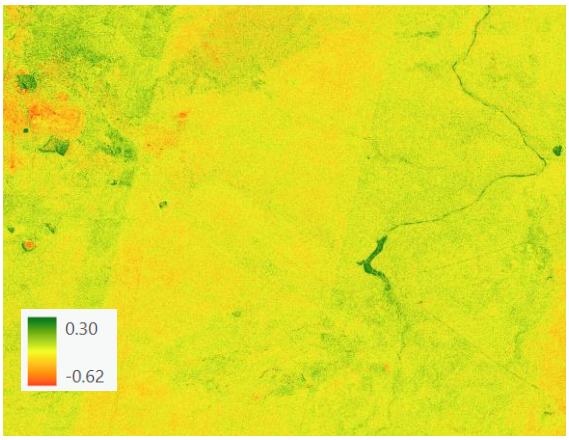
Change detection of remote sensing indexes before and after the failure events was conducted. The Jagersfontein tailings dam failure occurred on September 11, 2022. The imageries on September 4, 2022, and September 9, 2022, were used to detect change before the failure. As shown in Fig 3(a)(c)(e)(g)(i), remote sensing indexes do not have a noticeable change for the two dates before the 2022 Jagersfontein tailings dam failure event. Furthermore, we utilized the imageries on September 9, 2022, and September 12, 2022, in the change detection of the Jagersfontein tailings dam failure. Fig 3(b)(d)(f)(h)(j) illustrate that the change of remote sensing indexes can reveal the traveling path of the fluidized mass caused by the Jagersfontein tailings dam failure visibly. The Córrego de Feijão tailings dam failed on January 25, 2019. Imagery from December 20, 2018, and January 24, 2019, was used for the change detection before the failure. There was no significant change in remote sensing indexes before the 2019 failure, as shown in Fig 4(a)(c)(e)(g)(i). The imageries on January 24, 2019, and February 01, 2019, were utilized in the change detection for the Córrego de Feijão tailings dam failure incident. Fig 4(b)(d)(f)(h)(j) demonstrate that the change of remote sensing indexes can detect the tailings dam failure.



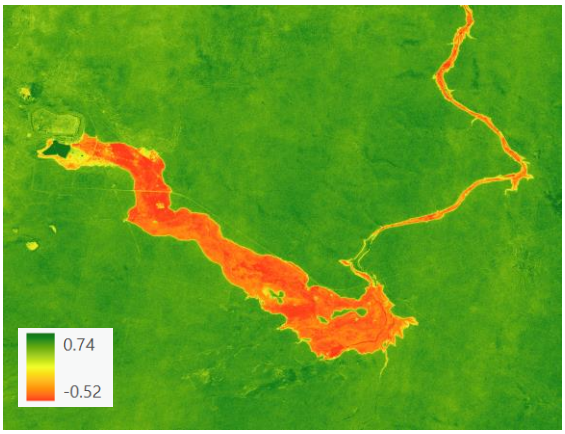

*(a) Before failure event- NDVI*



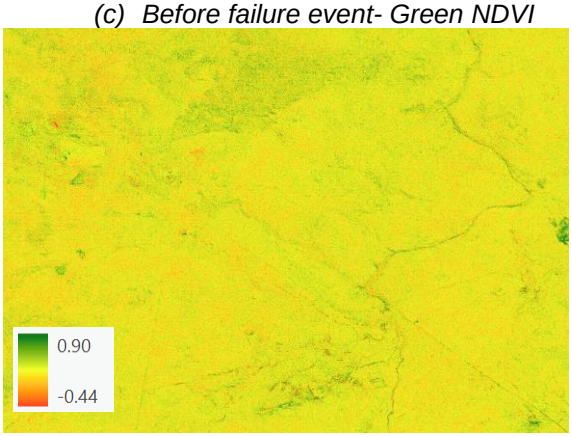

*(b) Failure event- NDVI*



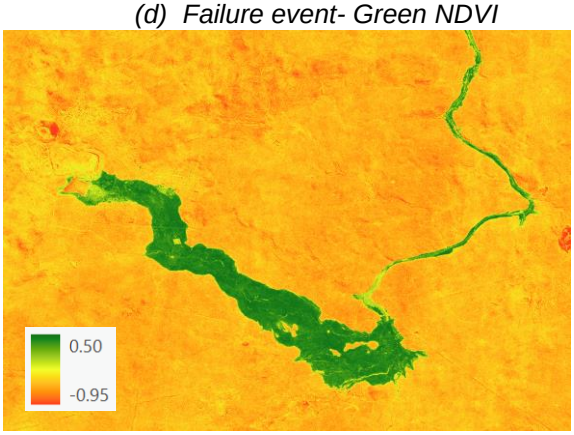

*(c) Before failure event- Green NDVI*



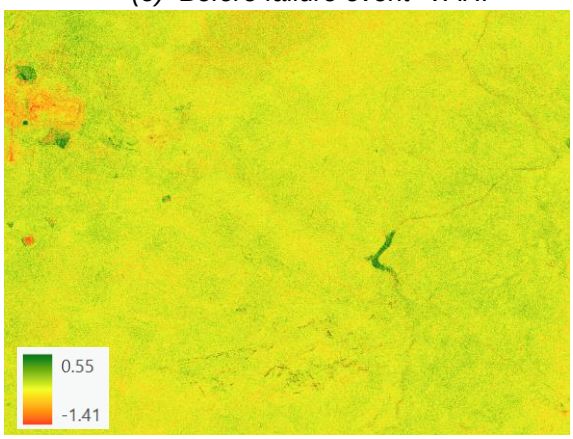

*(d) Failure event- Green NDVI*



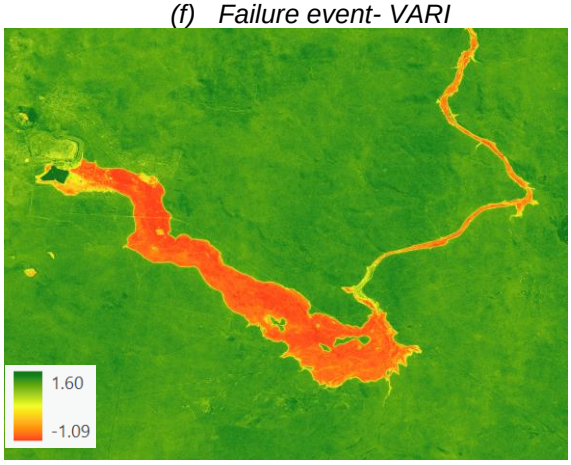

*(e) Before failure event- VARI*



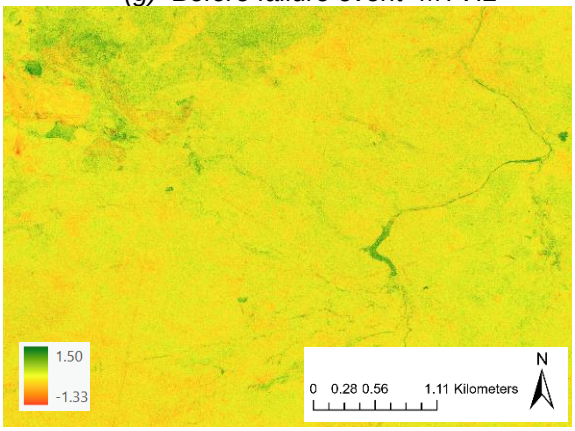

*(f) Failure event- VARI*



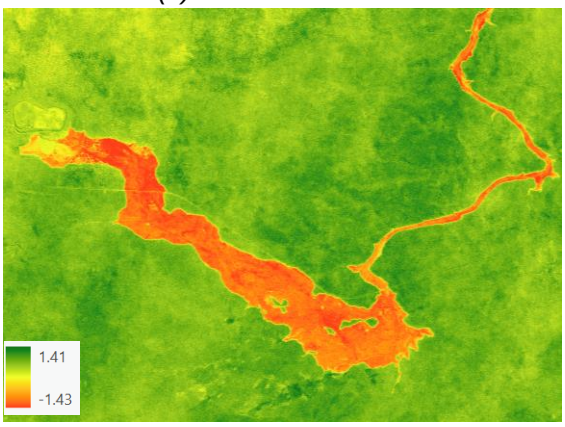

*(g) Before failure event- MTVI2*




*(h) Failure event- MTVI2*

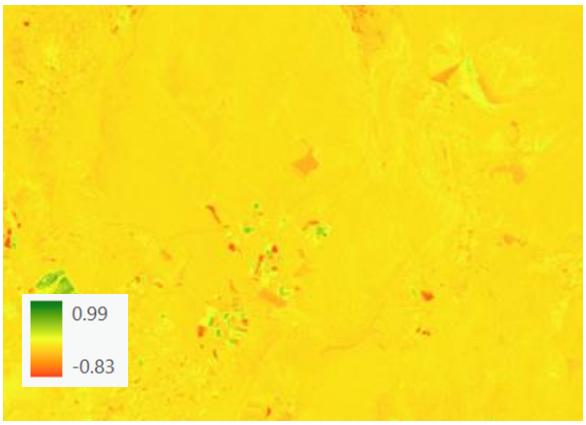



*(i) Before failure event- IO*

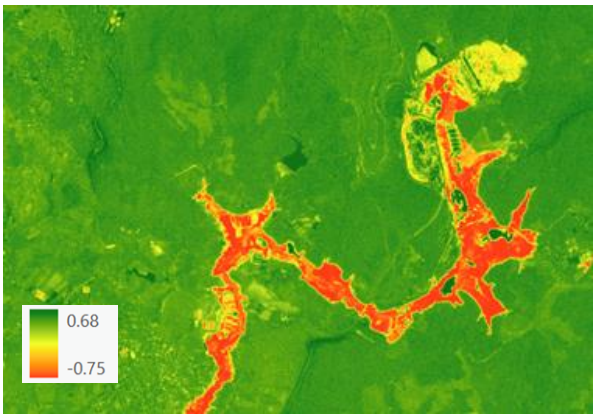



*(j) Failure event- IO*

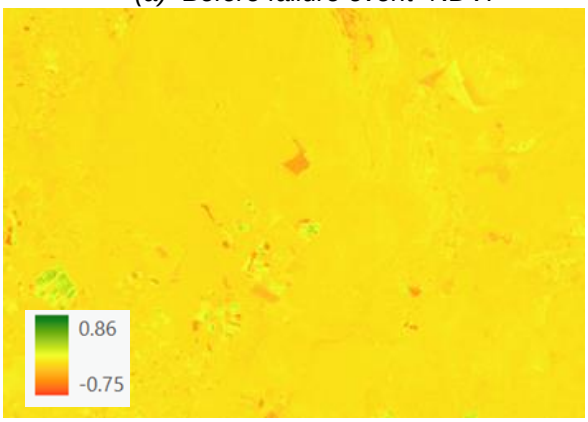
***Figure 3.*** *Change detection of remote sensing indexes- 2022 Jagersfontein tailings dam failure*



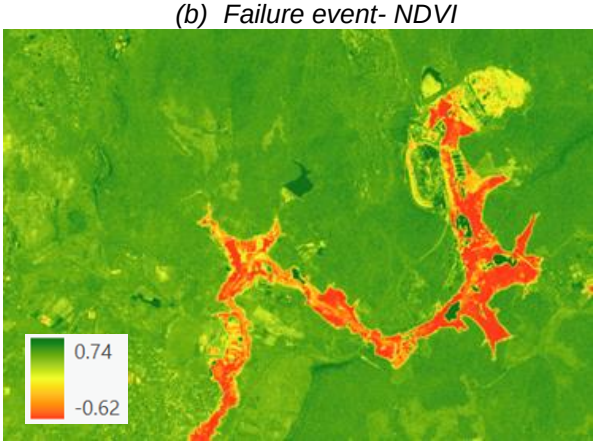

(a) Before failure event- NDVI



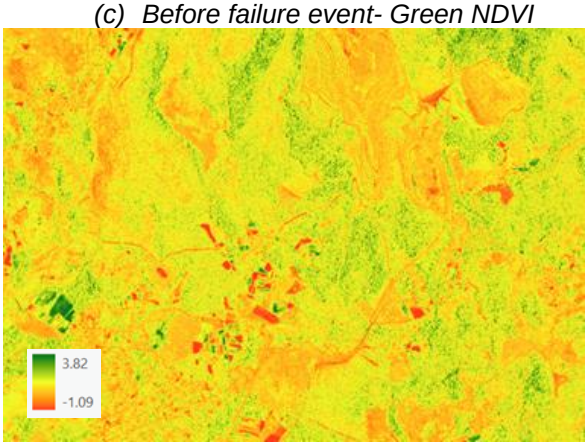

(b) Failure event- NDVI



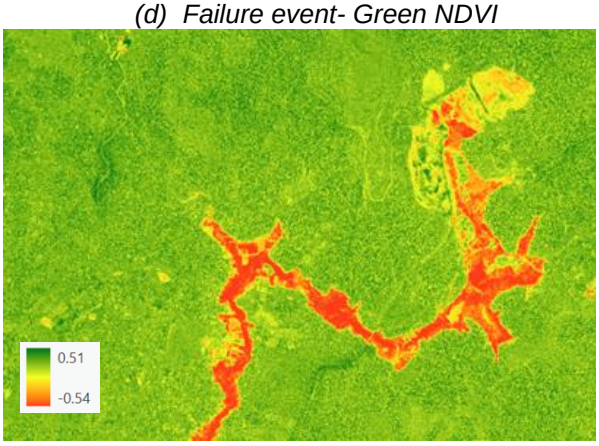

(c) Before failure event- Green NDVI



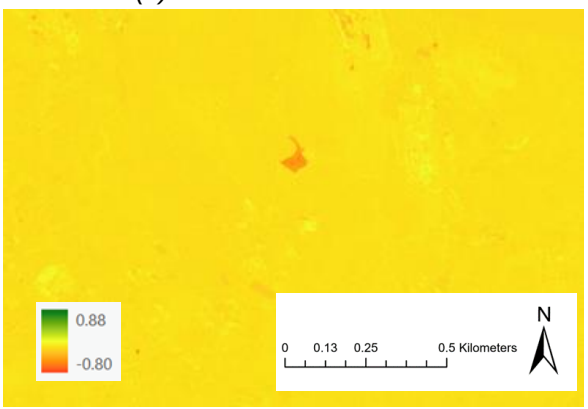

(d) Failure event- Green NDVI



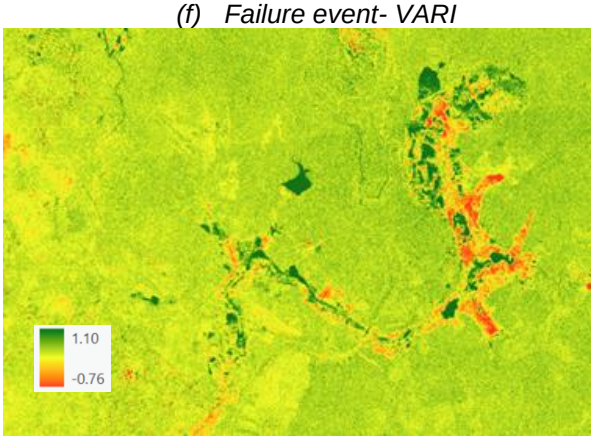

(e) Before failure event- VARI



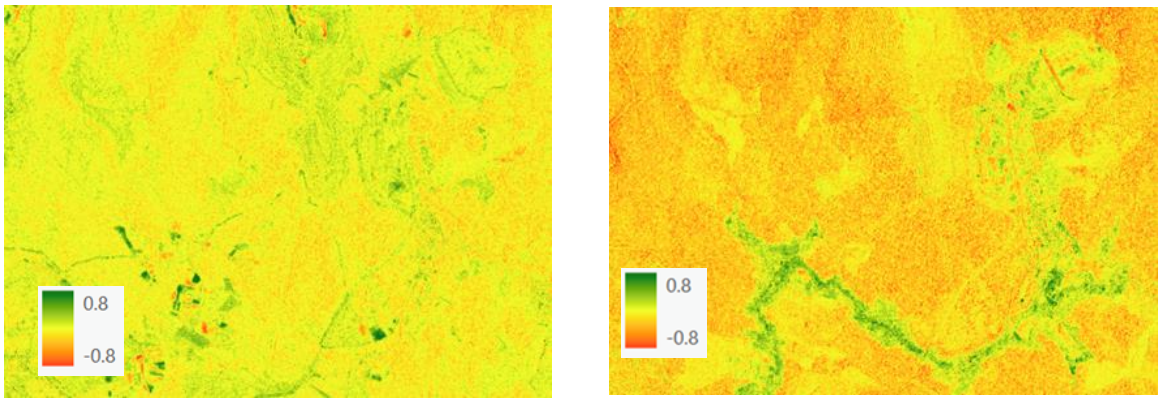

(f) Failure event- VARI




(g) Before failure event- MTVI2




(h) Failure event- MTVI2

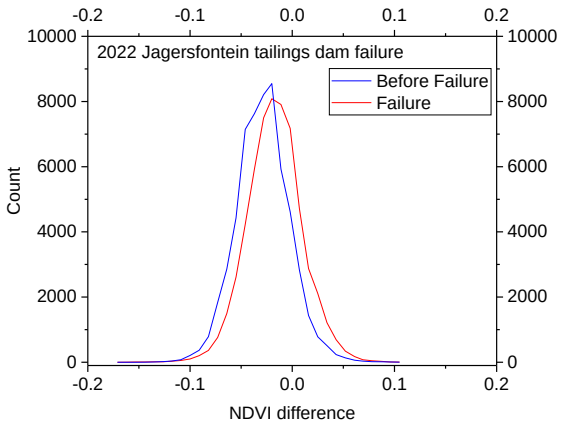



*(i) Before failure event- IO* *(j) Failure event- IO*

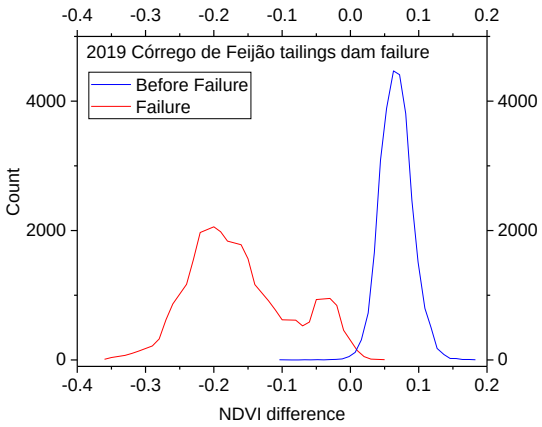
***Figure 4.*** *Change detection of remote sensing indexes- 2019 Córrego de Feijão tailings dam failure*

The change detection of remote sensing indexes can reveal the traveling path of the tailing plume, as shown in Fig 3 and 4. Since we cannot predict where and how large the surrounding area of a tailings plume will be before the tailings dam failure, we focus on the monitoring of remote sensing indexes within the tailings dams. Fig 5 includes distribution curves of remote sensing index difference within the tailings dam, as identified in Fig 1(b) and 2(b) as dashed polygon lines, before and after the failure events. Fig 5(a) displays that the mode of NDVI difference does not change significantly due to the 2022 Jagersfontein tailings dam failure. However, the mode of NDVI difference shifts from 0.06 to -0.2 due to the 2019 Córrego de Feijão tailings dam failure, as shown in Fig 5(b). The 2022 Jagersfontein tailings dam failure led to less than 0.01 change in the mode of Green NDVI difference, as presented in Fig 5(c). For the Córrego de Feijão tailings dam, the mode of Green NDVI difference moves from 0.07 to -0.15 because of the 2019 failure event, as shown in Fig 5(d). In Fig 5(e), Jagersfontein tailings dam has a 0.03 change in the mode of VARI difference due to the 2022 failure incident. The mode of VARI difference moves from 0.01 to -0.12 because of the 2019 Córrego de Feijão tailings dam collapse, as shown in Fig 5(f). Fig 5(g) indicates that the mode of MTVI2 difference has a change of 0.07 due to the 2022 Jagersfontein tailings dam failure incident. The mode of MTVI2 difference decreases from 0.06 to -0.01 because of the 2019 Córrego de Feijão tailings dam failure, exhibited in Fig 5(h). The 2022 Jagersfontein tailings dam failure brings about a 0.02 change in the mode of IO difference in Fig 5(i). A 0.17 change in the mode of IO difference occurs in the 2019 Córrego de Feijão tailings dam failure, displayed in Fig 5(j).

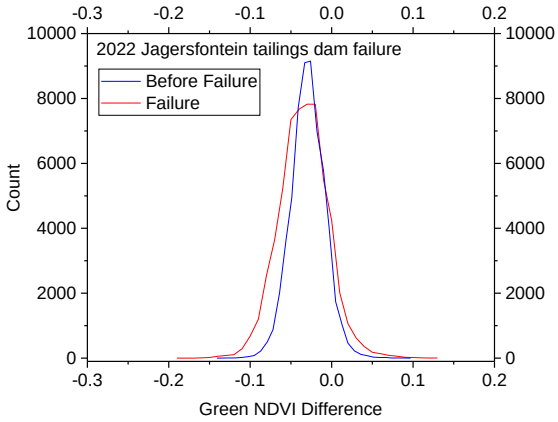
The Jagersfontein tailings dam is in a barren area and lacks vegetation (as shown in Fig 1). Therefore, a significant change in remote sensing indexes is not observed within the tailings dam before and after the failure. On the contrary, the Córrego de Feijão tailings dam is located in a heavily vegetated area. Fig 5(b)(d)(f)(h)(j) show that the change of remote sensing indexes difference within the tailings dam is notable and can be a clear sign of failure. When the Córrego de Feijão tailings dam collapsed, there was around or more than 0.2 change in the mode of NDVI, Green NDVI, and IO difference within the tailings dam. However, all remote sensing indexes differences for the Jagersfontein tailings dam failure event had less than 0.1 change.



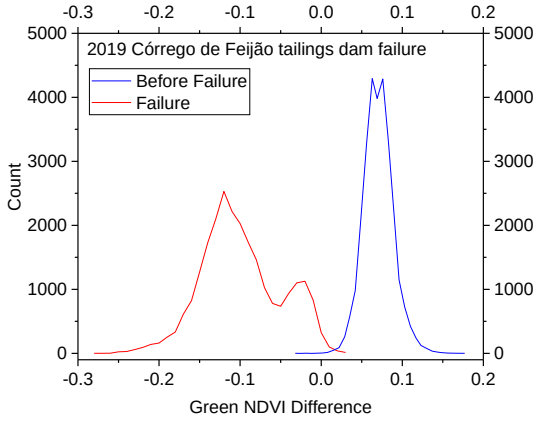

*(a) 2022 Jagersfontein tailings dam failure- NDVI*



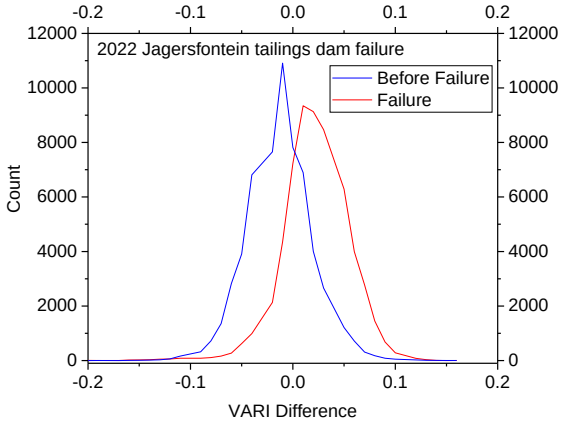

*(b) 2019 Córrego de Feijão tailings dam failure- NDVI*



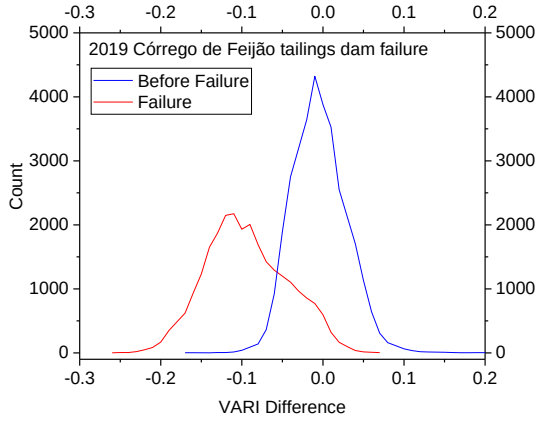

*(c) 2022 Jagersfontein tailings dam failure- Green NDVI*



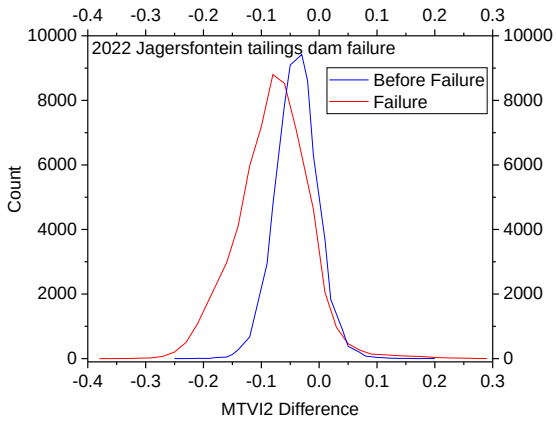

*(d) 2019 Córrego de Feijão tailings dam failure- Green NDVI*



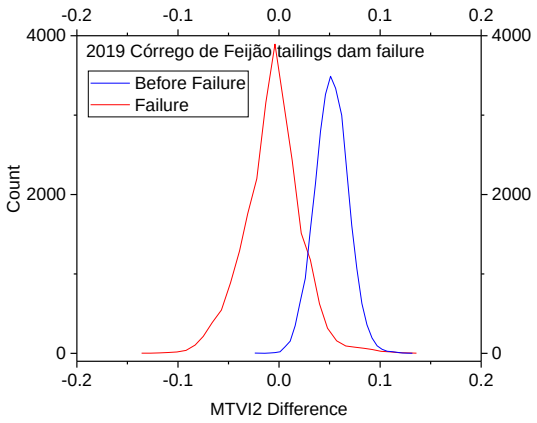

*(e) 2022 Jagersfontein tailings dam failure- VARI*



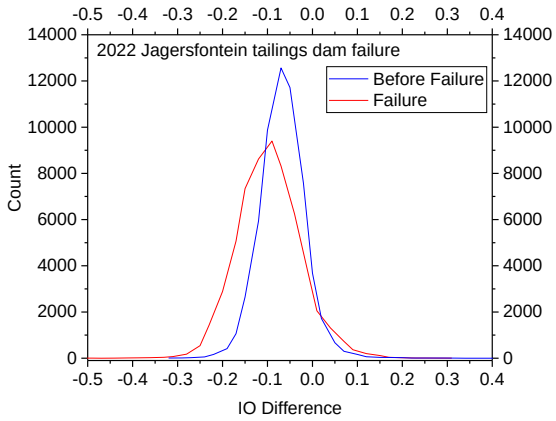

*(f) 2019 Córrego de Feijão tailings dam failure- VARI*



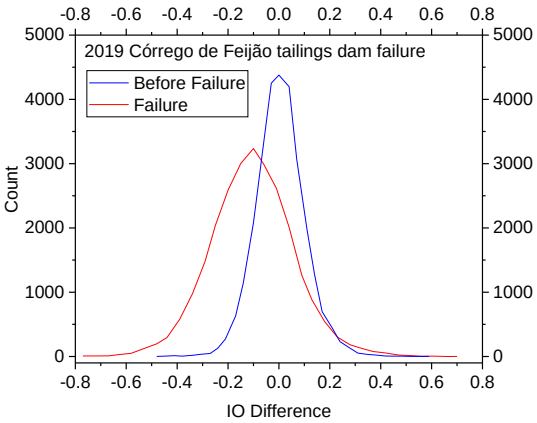

*(g) 2022 Jagersfontein tailings dam failure- MTVI2*




*(h) 2019 Córrego de Feijão tailings dam failure- MTVI2*




*(i) 2022 Jagersfontein tailings dam failure- IO*




*(j) 2019 Córrego de Feijão tailings dam failure- IO*

***Figure 5.*** *Remote sensing indexes differences before and after the failure event in the source*

## 4 CONCLUSIONS

Tailings dam failures can happen anytime during the operation or several years after mining activities have stopped and may reoccur in the same location. Therefore, tailings dams need regular maintenance and monitoring to ensure dams' stability. Daily high-resolution satellite data allows monitoring of tailings dam failures efficiently and economically in short intervals. Change detection analyses were conducted using vegetation and geological indexes for two recent failures in the 2022 Jagersfontein tailings dam failure and the 2019 Córrego de Feijão tailings dam failure event. It is shown that remote sensing indexes can be promising indicators of tailings dam failure, especially in vegetated mining sites. The Córrego de Feijão tailings dam is in a vegetated area, and the mode of all remote sensing indexes differences have more than 0.1 change within the tailings dam due to the 2019 failure incident. Among all indexes, the Normalized Difference Vegetation Index (NDVI) has the most significant change value of 0.26. In contrast, for the Jagersfontein tailings dam that is located in a non-vegetated area, no more than 0.1 change of remote sensing index difference is observed within the tailings dam. The threshold value of indexes can be applied as a reference of failure and assist the mining industry and supervisory boards in enhancing monitoring, safety management, and planning during and after mining operations.

## 5 ACKNOWLEDGEMENTS

The authors appreciate the financial support from NASA under Grant No. 18-DISASTER18-0022 and Jane Lewis Fellowship for this research. Any opinions, findings, conclusions, or recommendations expressed in this material are those of the author(s). They do not necessarily reflect the views of NASA or the Jane Lewis Fellowship program.

## REFERENCES


Azam, S., & Li, Q. (2010). Tailings dam failures: a review of the last one hundred years. Geotechnical news, 28(4), 50-54.

Bowker, L. N., & Chambers, D. M. (2015). The risk, public liability, & economics of tailings storage facility failures. Earthwork Act, 24, 1-56.

Bowker, L. N., & Chambers, D. M. (2017). In the dark shadow of the supercycle, tailings failure risk & public liability reach all time highs. Environments, 4(4), 75.

Dogan, H. M. (2009). Mineral composite assessment of Kelkit River Basin in Turkey by means of remote sensing. Journal of Earth System Science, 118, 701-710.

Grebby, S., Sowter, A., Gluyas, J., Toll, D., Gee, D., Athab, A., & Girindran, R. (2021). Advanced analysis of satellite data reveals ground deformation precursors to the Brumadinho Tailings Dam collapse. Communications Earth & Environment, 2(1), 1-9.

Haboudane, D., Miller, J. R., Pattey, E., Zarco-Tejada, P. J., & Strachan, I. B. (2004). Hyperspectral vegetation indices and novel algorithms for predicting green LAI of crop canopies: Modeling and validation in the context of precision agriculture. Remote sensing of environment, 90(3), 337-352.

Islam, K., & Murakami, S. (2021). Global-scale impact analysis of mine tailings dam failures: 1915–2020. Global environmental change, 70, 102361.

Kossoff, D., Dubbin, W. E., Alfredsson, M., Edwards, S. J., Macklin, M. G., & Hudson-Edwards, K. A. (2014). Mine tailings dams: Characteristics, failure, environmental impacts, and remediation. Applied Geochemistry, 51, 229-245.

Lyu, Z., Chai, J., Xu, Z., Qin, Y., & Cao, J. (2019). A comprehensive review on reasons for tailings dam failures based on case history. Advances in Civil Engineering, 2019.

Metternicht, G., Hurni, L., & Gogu, R. (2005). Remote sensing of landslides: An analysis of the potential contribution to geo-spatial systems for hazard assessment in mountainous environments. Remote sensing of Environment, 98(2-3), 284-303.

Moges, S. M., Raun, W. R., Mullen, R. W., Freeman, K. W., Johnson, G. V., & Solie, J. B. (2005). Evaluation of green, red, and near infrared bands for predicting winter wheat biomass, nitrogen uptake, and final grain yield. Journal of plant nutrition, 27(8), 1431-1441.

Mura, J. C., Gama, F. F., Paradella, W. R., Negrão, P., Carneiro, S., De Oliveira, C. G., & Brandão, W. S. (2018). Monitoring the vulnerability of the dam and dikes in Germano iron mining area after the collapse of the tailings dam of Fundão (Mariana-MG, Brazil) using DInSAR techniques with TerraSAR-X data. Remote Sensing, 10(10), 1507.

NASA Earth Observatory (2022). Jagersfontein Covered in Mining Waste. https://earthobservatory.nasa.gov/images/150497/jagersfontein-covered-in-mining-waste (Accessed February 8, 2023).

Owen, J. R., Kemp, D., Lébre, É., Svobodova, K., & Murillo, G. P. (2020). Catastrophic tailings dam failures and disaster risk disclosure. International journal of disaster risk reduction, 42, 101361.

Pettorelli, N. (2013). The normalized difference vegetation index. Oxford University Press.

Planet Team (2017). Planet Application Program Interface: In Space for Life on Earth. San Francisco, CA.

Rauhala, A., Tuomela, A., Davids, C., & Rossi, P. M. (2017). UAV remote sensing surveillance of a mine tailings impoundment in sub-arctic conditions. Remote sensing, 9(12), 1318.

Rico, M., Benito, G., Salgueiro, A. R., Díez-Herrero, A., & Pereira, H. G. (2008). Reported tailings dam failures: a review of the European incidents in the worldwide context. Journal of hazardous materials, 152(2), 846-852.

Robertson, P. K., De Melo, L., Williams, D. J., & Wilson, G. W. (2019). Report of the expert panel on the technical causes of the failure of Feijão Dam I. Commissioned by Vale, 81.

Rudorff, N., Rudorff, C. M., Kampel, M., & Ortiz, G. (2018). Remote sensing monitoring of the impact of a major mining wastewater disaster on the turbidity of the Doce River plume off the eastern Brazilian coast. ISPRS Journal of Photogrammetry and Remote Sensing, 145, 349-361.

Stow, D., Niphadkar, M., & Kaiser, J. (2005). MODIS-derived visible atmospherically resistant index for monitoring chaparral moisture content. International journal of remote sensing, 26(17), 3867-3873.

Streeter, E. W. (1892). Precious stones and gems: Their history, sources and characteristics. G. Bell & Sons.

Villarroel, L. F., Miller, J. R., Lechler, P. J., & Germanoski, D. (2006). Lead, zinc, and antimony contamination of the Rio Chilco-Rio Tupiza drainage system, Southern Bolivia. Environmental Geology, 51(2), 283-299.

Yangon, C. D. (2020). Mining disasters continue in Myanmar despite regulations [WWW Document]. URL https://www.dw.com/en/mining-disasters-continue-in-myanmar-despite-regulations/a-54042106 (accessed 12.26.2022).